Energy Nexus 17 (2025) 100377

Contents lists available at ScienceDirect

Energy Nexus

journal homepage: www.elsevier.com/locate/nexus

Full Length Article

Kinetic and thermodynamic insights into sewage sludge torrefaction: Energetic optimization and safety considerations

Blanca Castells [a,b,*], Roberto Paredes [a], David León [a,b], Isabel Amez [a,b]

[a] E.T.S. Ingenieros de Minas y Energía, Universidad Politécnica de Madrid, Ríos Rosas 21, 28003, Madrid, Spain
[b] Tecnological Center TECMINERGY and Laboratorio Oficial J.M. Madariaga (LOM), Universidad Politécnica de Madrid, Madrid, Spain

ARTICLE INFO

Keywords:
Torrefaction
Thermogravimetric analysis
Biomass
Differential scanning calorimetry
Kinetic analysis
Self-ignition risk

ABSTRACT

In the current energetic scenario, biofuels play a crucial role, with torrefaction being one of the most popular pretreatments as it significantly reduces the main disadvantages of these fuels. This study provides novel insights into torrefied sewage sludge as a solid biofuel by examining both the energetic conversion process and associated safety issues. To do so, torrefaction was carried out at three different temperatures (220 °C, 250 °C, and 300 °C) and two residence times (30 and 60 min), resulting in seven distinct samples. These samples underwent proximate analysis, thermogravimetric analysis (TGA), and differential scanning calorimetry (DSC) in air, nitrogen, and oxygen atmospheres to simulate combustion, pyrolysis, and determine heating values respectively. The analysis reveals that torrefaction at 300 °C for 60 min produces the best results, enhancing the higher heating value (HHV) by 6% and increasing reaction heat by 16%. Additionally, we observed lower pyrolysis activation energies in samples torrefied for 30 min compared to 60 min. The kinetic parameters were meticulously evaluated, showing a clear relationship between torrefaction parameters and pyrolysis activation energy. For instance, the activation energy (*Ea*) for raw sewage sludge was found to be between 338.02 kJ/mol and 375.43 kJ/mol. In contrast, torrefied samples showed reduced *Ea* values mostly under 300 kJ/mol. For the first time, we assessed self-ignition risk through TGA, finding that while most samples exhibit low risk, the increased heating value from torrefaction does elevate this risk. This comprehensive evaluation not only advances the understanding of sewage sludge torrefaction but also offers a practical framework for integrating biofuels into sustainable energy systems, supporting global efforts toward cleaner energy transitions.

1. Introduction

Climate change is a critical issue that requires immediate attention and action. One of the key drivers of climate change is the over-reliance on non-renewable sources of energy, such as coal, oil, and gas, which emit greenhouse gases when burned. Renewable energy sources, such as biomass, are becoming increasingly important in the fight against climate change [1–3]. Biomass is organic matter, such as wood, crops, and waste, that can be used to generate energy. Unlike fossil fuels, biomass is a renewable resource that can be replenished and is carbon neutral, meaning it does not release more carbon dioxide into the atmosphere than it absorbs [4]. Utilizing biomass as a source of energy can help reduce our reliance on non-renewable sources of energy and decrease our carbon footprint, making it a crucial part of the transition to a more sustainable future [5–7]. Biomass can be obtained from different wastes, such as agriculture, forestry, food industry, and even sewage sludge [8].

Sewage sludge is a by-product of wastewater treatment processes that contains high levels of organic matter and nutrients. However, its disposal has become a major environmental concern due to its high moisture content, potential pathogenic microorganisms, and heavy metal content [9]. Therefore, developing sustainable and effective methods for sewage sludge management is essential [10].

Torrefaction is a thermal treatment process that has proved to improve biomass properties to be used as fuels [11]. Torrefaction can be used to convert sewage sludge into a solid, stable, and energy-dense product that can be used as a fuel or soil amendment [12]. During torrefaction, sewage sludge is heated to a temperature of 200–300 °C in an oxygen-free environment, resulting in the removal of water, carbon monoxide and dioxide, sulphur compounds and volatile organic compounds [13–15]. The resulting product, known as biochar, has a high carbon content and low ash content, making it an attractive alternative

* Corresponding author.
E-mail address: b.castells@upm.es (B. Castells).

https://doi.org/10.1016/j.nexus.2025.100377
Received 12 September 2024; Received in revised form 5 December 2024; Accepted 8 February 2025
Available online 9 February 2025

to fossil fuels. Although biochar is the main product from torrefaction, this process also produces liquid and gaseous byproducts. The liquid product primarily consists of water and organic compounds, such as acids and phenols [16,17].On the other hand, the gaseous fraction, often contains combustible components such as methane and hydrogen, although the main components are carbon oxides [16].

Previous studies have shown that sewage sludge torrefaction can reduce the volume and weight of the waste, increase its heating value, and improve its storage and handling properties [18,19]. Moreover, the resulting biochar can be used to improve soil quality and reduce greenhouse gas (GHG) emissions [20,21]. Sewage sludge can be used in for co-firing in thermal power plants, reducing GHG emissions and dependency on fossil fuels [22,23]. Furthermore, according to Trop et al. [24], torrefied sewage sludge can be used in co-gasification processes and can outperform coal. As the growing production of sewage sludge poses significant waste management challenges, torrefaction offers a sustainable solution by converting sludge into a stable, energy-dense biofuel, that can be used in heat generation systems, and gasification and pyrolysis feedstock [25,26].

To understand the thermal behaviour of sewage sludge several authors have used thermoanalytical techniques such as thermogravimetric analysis, simultaneous thermal analysis or differential scanning calorimetry [27–31]. Although some authors research focused on using these techniques to address torrefaction kinetic [12,32,33], most of the previously published literature focus on kinetic analysis of combustion and pyrolysis processes. It was found that pyrolysis process took place at temperatures lower than 550 °C [34] and three different stages took place: between 180 and 220 °C evaporation, between 220 and 650 °C main decomposition and between 650 and 800 °C final decomposition [28,35]. Regarding activation energy values, high values were obtained, over 300 kJ/mol [36]. Kinetic analysis is critical for understanding combustion and pyrolysis processes in biomass as it provides fundamental insights into the reaction mechanisms, rates, and energy requirements of thermal degradation. Activation energy and pre-exponential factor describe how quickly biomass decomposes under specific thermal conditions, therefore a proper understanding of these parameters contributes to the understanding not only of the reaction mechanisms but also to the process optimization, and energy requirements [37–40]. Nevertheless, there is a gap in literature regarding pyrolysis kinetics of torrefied sewage sludge, that addresses how different torrefaction conditions affect the pyrolysis process.

Moreover, from the kinetic results it is also possible to define the thermodynamic parameters such as enthalpy, entropy and Gibbs free energy, which contributes to the complete understanding of the thermodynamic reactions that takes place [41,42]. Some authors have applied these methods to define these thermodynamic parameters to sewage sludge [43] and to characterize torrefaction process [44,45]. However, there is a lack of literature regarding the thermodynamic and kinetic parameters of torrefied sewage sludge.

Even if torrefaction significantly improves sewage sludge properties, the effect of torrefaction on the nutrient content of the sludge and the fate of the remaining heavy metals is still under investigation [46]. Moreover, torrefaction might increase ignition risk [47] Because of that, self-ignition tendency has to be addressed by assuring that torrefied samples are below their self-ignition temperature [48]. Also, Arriola et al. [49], pointed out that biochar self-ignition affects the energy yield. Torrefaction process not only modifies composition but also ignition temperatures and burning rates which have a direct effect on the ignition risks [50,51]. Specifically, some authors have already researched on this topic, finding out that sewage sludge presents a considerable self-ignition risk [52,53].

Although several authors have researched sewage sludge torrefaction, there is little literature that properly assess the effect of torrefaction temperature and residence time both in energetic parameters and self-ignition risk. Because of that the present study intends to address sewage sludge torrefaction by using TGA and DSC techniques, addressing this gap in scientific literature and providing unique insights into the thermal behaviour, reaction kinetics, and energetic properties of the samples. Results regarding the effect of torrefaction temperature and residence time in the physicochemical properties of sewage sludge are reported. Pyrolysis kinetic parameters for samples torrefied at different temperatures and times are defined together with the evaluation of the heating value, and the thermodynamic parameters. Furthermore, self-ignition risk is assessed using two different methods in order to properly study the industrial safety problems that might be associated with the use of torrefied sewage sludge. The inclusion of self-ignition risk analysis offers a novel perspective, addressing practical concerns for the safe handling and storage of torrefied products.

Overall, this study differentiates itself from previous works on sewage sludge torrefaction by adopting a comprehensive approach that integrates both energetic optimization and safety considerations. Prior studies focused mainly on the energetic enhancements of torrefaction, while the present research explores the self-ignition risks associated with torrefied sewage sludge. These aspects contribute both to the scientific understanding and the practical applications of sewage sludge as a biofuel.

2. Materials and methods

2.1. Torrefaction and samples characterization

The present study used sewage sludge obtained from a company located in Madrid (Spain) dedicated to industrial cleaning. The sample was thermally dried in the premises of the company. Sample particle size was determined using a Malvern Mastersizer 2000 apparatus, found out that the median particle size was 98.1 μm. As mentioned before, sewage sludge presents several disadvantages that reduce its use as a fuel. Because of that, the sample was submitted to different torrefaction processes.

Before the torrefaction process, the sample was dried at 105 °C during 24 h. After that, 30 ± 5 g of sample is inserted in the torrefaction reactor which is a hermetic container with an inlet and outlet gas. The inlet is connected to a nitrogen flow and the outlet to an oxygen analyser. When the oxygen inside the reactor is lower than 0.1% the outlet is closed. In order to produce a slight overpressure that helps the hermetic closing of the rector, the inlet is closed a few seconds later than the outlet.

Once that the inert atmosphere is achieved, the reactor is placed inside an oven set at the torrefaction temperature. The reactor remains inside the oven during the residence time, and afterwards the sample is removed from the reactor. The present study has used three different temperatures: 220 °C, 250 °C and 300 °C, and two different residence times: 30 and 60 min. Torrefaction temperatures and residence times were selected in order to be able to see the differences in the degradation process, and the energetic density increase. These parameters were defined according to previously published literature [54,55]. A thermocouple was placed inside the torrefaction reactor measuring the atmosphere temperature inside the reactor. However, this thermocouple is not in contact with the sample and, therefore, it has to be considered that the sample might take some time to reach torrefaction temperature, consequently, the effective residence time might be lower than the theoretical time, as once that the reactor is inserted in the oven the residence time countdown begins, however, the sample does not reach the torrefaction temperature immediately. Nevertheless, according to the thermocouple records, the temperature inside the torrefaction reactor did not require in any test more than 5 min to reach the furnace temperature. Because of that, it is considered that similar time is required by the sample to reach the torrefaction temperature.

Proximate analysis was carried out in each sample in order to properly characterize the samples. European standards EN ISO 18122 and EN ISO 18123 were used for moisture and volatile matter determination, while ash content was obtained using ISO 1171:2024 to

perform the test at higher temperatures and assure the complete volatilization of the organic compounds. Table 1 presents these results for each sample, which is identified by its torrefaction temperature (T) and residence time (t).

2.2. Thermogravimetric analysis (TGA)

Thermogravimetric analysis (TGA) was carried out using a Mettler Toledo TG/DSC T50 apparatus. Several tests were carried out using different atmospheres and heating rates but maintaining sample mass (55 ± 5 mg) and initial and final temperature (from 30 °C to 800 °C). Three different atmospheres were used depending on the use of the results: nitrogen, air, or oxygen. Nevertheless, in all the test gas flow was set at 50 mL/min. Again, heating rate (β) selection depended on the use of the results, which lead to use several heating rates: 3, 5, 7, 10 and 20 K/min. These specific heating rates were selected in order to perform the self-ignition tendency methodology proposed by Jankovic et al. (2020) [56].

2.3. Differential scanning calorimetry (DSC)

The same apparatus that was used to carry out thermogravimetric analysis, allows to fulfil differential scanning calorimetry (DSC). In the present study, DSC was carried out using a 50 mL/min oxygen flow atmosphere with a constant heating rate of 5 K/min, as heating rates greater than 5 K/min might lead to thermal lag [57,58] Initial temperature was set at 30 °C and final temperature at 700 °C. Due to the fast oxidation that takes place, DSC records a peak when most of the samples volatile matter releases. Therefore, if the area under this peak is calculated, it can provide information regarding the energetic value of the sample. Furthermore, in order to contrast the data provided from this analysis, an estimation of the high heating value (HHV) was carried out using the model proposed by Estiati et al. [59] The model applies proximate analysis results to the following equation (Eq. (1)):

$$HHV = 0.3241FC + 3.7667{\cdot}10^{-4}FC^2 - 4.1530{\cdot}10^{-4}FC{\cdot}V + 0.1947\ V - 2.820{\cdot}10^{-4}V^2 - 0.0025\ A \quad (1)$$

Where *HHV* is the estimation of the high heating value (MJ/kg), *FC* is the fixed carbon content (%), *V* is the volatile matter (%) and *A* represents the ash content (%).

Although there are several models to estimate HHV, the one defined by [59] was chosen in the present study mainly due to two reasons. First of all, the simplicity of the model, as the estimation is carried out using only proximate analysis data which reduces the number of tests needed. The second reason is the accuracy of the model, as it has been proved that the results obtained using this method are highly reliable for biomass [60].

2.4. Kinetic analysis

Besides providing information regarding the thermal behaviour of the samples, TGA allows to define the kinetic parameters of the reaction.

Table 1
Samples proximate analysis.

	Ash (%) d.b.	Volatile (%) d.b.	Moisture (%)	Fixed Carbon (%) d.b.
Raw	25.42	58.23	8.18	16.34
T220t30	30.50	51.24	1.07	18.26
T220t60	34.39	42.31	1.47	23.30
T250t30	27.64	55.34	1.58	17.02
T250t60	28.55	51.05	1.18	20.40
T300t30	27.38	51.93	0.99	20.69
T300t60	27.93	47.27	0.97	24.81

Therefore, pyrolysis reaction was stimulated by applying nitrogen flow. There are several kinetic models that allow the determination of the activation energy (*Ea*) and the preexponential factor (*A*) [61], from which isoconversional methods (also known as model free methods) have proved to provide the most reliable information [62] as they do not make assumptions regarding the reaction mechanism. Because of that, the present study applied KAS, FWO and Friedmann methods [63–66]. To do so, it is necessary to perform each analysis using at least three different heating rates, which were set at 5, 10 and 20 K/min. Each test was repeated twice and standard deviation (σ) between both tests was calculated. After that, the average value of the three standard deviations (one per heating rate) was calculated for each sample. This value is reported in the results section (see Table 6). When the standard deviation average value was greater than 2% the tests were repeated a third time. All the methods use the following thermochemical rate (Eq. (2)):

$$\frac{d\alpha}{dt} = k(t)f(\alpha) \quad (2)$$

Where α represents the conversion degree, t the time, $k(t)$ the reaction rate constant defined by using Arrhenius equation, and $f(\alpha)$ the reaction model. Therefore, the kinetic models will define the activation energy *(Ea)* for each conversion degree which can be defined as seen in Eq. (3):

$$\alpha = \frac{m_0 - m_t}{m_0 - m_f} \quad (3)$$

Where m_0 is the initial mass, m_t is the mass at a certain time t and m_f is the final mass. According to this definition, α is dimensionless and is between 0 and 1. For the preexponential factor, the following model-free non-isothermal equation (Eq. (4)) was used [67]:

$$A = \beta{\cdot}E_\alpha{\cdot}\exp\frac{E_\alpha}{R{\cdot}T_p}\Big/\ R{\cdot}T_p^2 \quad (4)$$

Where R is the universal gas constant and T_p is the peak temperature, which is the temperature at which the mass loss rate reaches its maximum.

2.5. Thermodynamic analysis

Upon defining the activation energy and the preexponential factor, it becomes feasible to approximate essential thermodynamic parameters, such as changes in enthalpy (ΔH, *kJ/mol*), Gibbs free energy (ΔG, *kJ/mol*), and entropy (ΔS, *kJ/mol · K*) [67,68]. One should take note that, due to their dependence on the activation energy, each parameter yielded three distinct values, aligning with the respective isoconversional methods. Furthermore, the equations display a reliance on both β and peak temperature T_p. Therefore, an average of these values was utilized. Table 2 presents the equations employed for defining the thermodynamic parameters (equations 5 to 7), where K_B symbolizes the Boltzmann constant with a value of $1.381{\bullet}10^{-23}$ J/K, h represents the Planck constant with a value of $6.626{\cdot}10^{-34}$ J•s, T denotes the absolute temperature in Kelvin (K), and T_p stands for the peak temperature observed on the DTG curve in Kelvin (K).

2.6. Self-ignition risk

As mentioned before, torrefaction does not only modify physicochemical biomass properties in terms of energy, but also might change

Table 2
Thermodynamic equations.

Entalpy	$\Delta H = E_\alpha - (R{\cdot}T)$	(5)
Gibbs free energy	$\Delta G = E_\alpha + R{\cdot}T_p{\cdot}l_n\left[\left(K_B{\cdot}T_p\right)/(h{\cdot}A)\right]$	(6)
Entropy	$\Delta S = \frac{\Delta H - \Delta G}{T_p}$	(7)

the associated risk. In the present study, two different methodologies have been used to address self-ignition risk.

Both methodologies use TGA data to classify the samples according to their self-ignition risk. The first one was described by García-Torrent et al. [53] and combines TGA results using air and oxygen atmosphere. In both tests, heating rate was set at 5 K/min. When oxygen flow is applied, a fast oxidation takes place that leads to a drastic mass drop at a certain temperature, which is called characteristic temperature (T_{char}). Graphically, this temperature is obtained as the temperature at which takes place the maximum peak in the DTG (first derivative of TGA) curve when applying oxygen atmosphere. On the other hand, when air atmosphere is applied, activation energy is calculated using Cumming's equation [69]. By plotting T_{char} vs Ea it is possible to classify the sample into four different areas: low, medium, high, and very high risk. It has to be noticed that the method uses the activation energy value obtained using a model fitting method that approximates the data to a first order reaction, which can lead to significant errors. Nevertheless, this self-ignition risk estimation has proved to be useful for samples comparison.

The second method applied is the one proposed by Jankovic et al. [56]. The method applies air atmosphere and five different heating rates: 3, 5, 7, 10 and 20 K/min. In this method a so-called "self-heating coefficient" ($coef$) is calculated using volatile matter, derivative thermogravimetric curve (DTG) and reference temperature (see Eq. (8)). Using DTG, heating rate and volatile matter it is possible to define the microscopic devolatilization rate (noted as ψ) and the self-heating coefficient (Eqs. (8) and (9)):

$$coef = \frac{DTG_i}{V \cdot \beta_{j,i}} \cdot T_{ref,i} \tag{8}$$

$$\psi = \frac{V \cdot \beta_{j,i}}{T_{ref,i}} \tag{9}$$

Where V represents the volatile matter, DTG_i is derivative thermogravimetric data for the i th point, $T_{ref,i}$ is the reference temperature of the i th point, and $\beta_{i,j}$ is the heating rate for the j th heating rate corresponding to each i th point. This coefficient is calculated for each heating rate and three different reference temperatures (i th points): start peak, inflection, and end peak.

Therefore, when the method is applied three different coefficients matching three different reference temperatures are obtained. When these points are plotted and a regression line is calculated, the slope of this line represents the so-called thermogravimetric index of spontaneous ignition (TG_{spi}), which can be defined as shown in Eq. (10):

$$TG_{spi} = slope \cdot \psi \tag{10}$$

Furthermore, this index classifies the spontaneous ignition potential according to Table 3:

3. Results and discussion

3.1. Torrefaction effects on physic-chemical properties

The results reported on Table 1 showed one of the most important improvements produced by torrefaction pre-treatment, which is the reduction of hygroscopicity [70]. The samples were tested several days after torrefaction process was carried out, which means that not only moisture content is significantly reduced, but also the samples do not absorb environmental moisture. The values were reduced up to ~1%, indeed, when applying temperatures of 300 °C moisture content is below 1%. However, no significant differences were noticed between torrefaction temperatures and residence times. Regarding the volatile content, T220t60 sample showed a significant decrease of volatile matter and increase of ash content. Nevertheless, proximate analysis tests were repeated three times (Table 1 reports average values); therefore, these data can be attributed to heterogeneity of the sample. Further studies should consider repeat torrefaction at this temperature and residence time in order to address the obtained results in the proximate analysis to understand why those conditions led to the lowest volatile content.

Table 3
Spontaneous ignition classification according to TG_{spi}.

TG_{spi}	Class
< 0.02	Non-reactive
0.02 – 0.03	Low reactive
0.03 – 0.05	Reactive
> 0.05	High reactive

On the other hand, according to previously published literature [71] temperatures and times do produce an effect on the mass yield. Indeed, the greater the torrefaction temperature and residence time, the lower the mass yield. In the present study mass yield for samples torrefied at 220 °C were 90.2% and 89.4% for 30 and 60 min residence time respectively, while at 250 °C decreased up to 87.9% and 84.5%, and for 300 °C reached 77.4% and 72.8%. Those results are consistent with previously published literature, and the higher mass loss recorded under the most severe torrefaction conditions is produced due to the moisture and volatile organic matter release [54,55]. Furthermore, the colour of the samples changed after torrefaction, as torrefied samples showed a darker colour: the higher the temperature, the darker the colour [72]. This effect is mainly produced due to moisture and light volatiles release [73].

Regarding TGA results, Fig. 1 shows TGA (a) and DTG (b) curves for each sample using air atmosphere and 5 K/min heating rates. These conditions were selected as 5 K/min reduces the thermal lag [74] and, therefore, it is possible to properly see the thermal degradation. The curves are plotted from 30 °C up to 800 °C as it is the dynamic segment in which the temperature is increased at 5 K/min. A 5 min isotherm at 800 °C was carried out after the test, however it is not included in the plots nor discussed as the mass does not vary in this segment and, therefore, it could not be included in the kinetic analysis. Fig. 1(a) shows that raw biomass presents the lower residue after TGA, as was also noticed when addressing ash content reported in Table 1, and also the greatest mass loss due to moisture release. Nevertheless, it has to be noted that the final mass after TGA (see Table 4 for precise values) is always greater than the ash content. At 800 °C, the degradation of fixed carbon and residual organic matter might not be fully complete, resulting in a higher residual mass than the ash content determined by standard ash determination methods, which also consider higher temperatures to ensure the complete combustion of organic components and the stabilization of inorganic residues. Samples torrefied at 220 °C still present a mass loss up to 200 °C which is not shown in the other samples. This fact means that torrefaction at this temperature reduces surface moisture, but intramolecular moisture remains. In Fig. 1(b) DTG curves show also this moisture release as a peak at the beginning of the process. After that, around 250 °C every sample shows a significant peak produced due to thermal degradation. In every curve, this peak presents a shoulder, which accounts a secondary volatile release and breakdown of more stable organic structures. Sewage sludge degradation process involves complex reactions primarily driven by the breakdown of proteins, lipids, and other organic fractions. The main peak in the DTG curve aligns with the decomposition of these major components, while the shoulder reflects subsequent reactions. Finally, at the end of the curves there is another peak for most of the samples, which might correspond to a carbonaceous matter decomposition [75].

In summary, the curves showed that there are three main degradation stages: first one up to 200 °C, second one from 200 °C up to 500–550 °C where most of the matter decomposes, and the last one from 550 °C until the end of the process. These stages are consistent with previously published literature and are produced due to dehydration and moisture

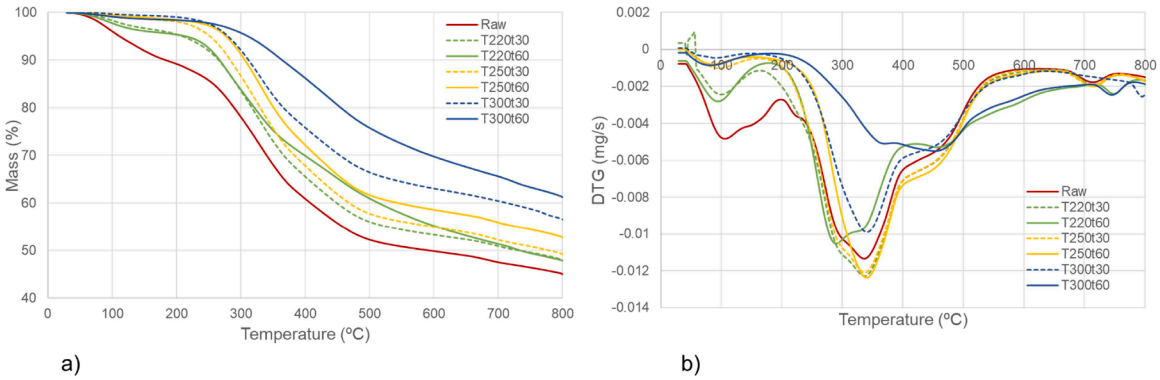

Fig. 1. TGA (a) and DTG (b) curves for each sample using air atmosphere and 5 K/min heating rate.

Table 4
TGA and DTG parameters.

Sample	TGA Final Mass (%)	DTG Peak Temperature (°C)	DTG Peak Intensity (mg/s)
Raw	45.0	−0.01134	336
T220t30	47.9	−0.01230	337
T220t60	47.8	−0.01051	289
T250t30	49.1	−0.01209	337
T250t60	52.6	−0.01237	337
T300t30	56.6	−0.00991	340
T300t60	61.2	−0.00548	454

release, main decomposition of carbohydrates and lipids and inorganic matter degradation respectively [28].

It can be noticed that when torrefaction temperature is increased the decomposition softens leading to a constant mass loss with less pronounced peaks. Some authors already pointed out that the mass loss produced during second phase, where carbohydrates and lipids decompose, is reduced when higher torrefaction temperatures are applied [76]. Indeed, if sample T300t60 is considered, it can be noticed that it presents the greatest residue after pyrolysis, as the devolatilization processes are less intense and the DTG curve presents the lower peaks. Table 4 shows the final residues after TGA and the DTG temperatures and peak intensities.

These results are consistent with previously published literature, as sewage sludge final mass after thermogravimetric analysis is usually greater than 40% and the main decomposition process takes place between 200 and 600 °C [18,61,77]. Miskolczi et al. [61] observed that the main decomposition reactions of sewage sludge present multiple stages attributed to the degradation of lipids, polysaccharides, and proteins. On the other hand, Świechowski et al. [77] reported multi-step thermal degradation for sewage sludge, emphasizing a prominent peak between 200 °C and 300 °C associated with hemicellulose decomposition, followed by a slower phase above 400 °C linked to lignin and residual fractions, which is not so clear in the results reported in Fig. 1. Nevertheless, two primary degradation stages are also present in these results: hemicellulose and cellulose decomposition below 400 °C and lignin degradation extending up to 500 °C. However, the distinct behaviour observed in the DTG curves, including the sharper peaks for certain torrefaction conditions, suggests potential catalytic effects from the sludge's inorganic constituents [10].

3.2. DSC and HHV

Fig. 2 shows the DSC peaks produced when a fast oxidation of the sample is produced. It can be noticed that all the samples' peaks (besides T300t60) are located around 350–375 °C, which means that this is the temperature at which the reaction fully grows. Indeed, this result is consistent with the DTG curves from Fig. 1(b), as the main mass loss is produced in this temperature range.

Most of the samples produced one main peak but also something similar to a shoulder or a smaller peak prior to it. It means that although the main reaction takes place between 350 and 400 °C, there is a previous matter decomposition that produces an exothermic reaction between 200 and 350 °C. However, sample T300t60 behaves completely different, as the main peak is produced around 250 °C and the second around 350 °C. As this sample was submitted to the most severe torrefaction conditions, it seems that the process has weaken the links between the molecules leading to lower temperatures to break these

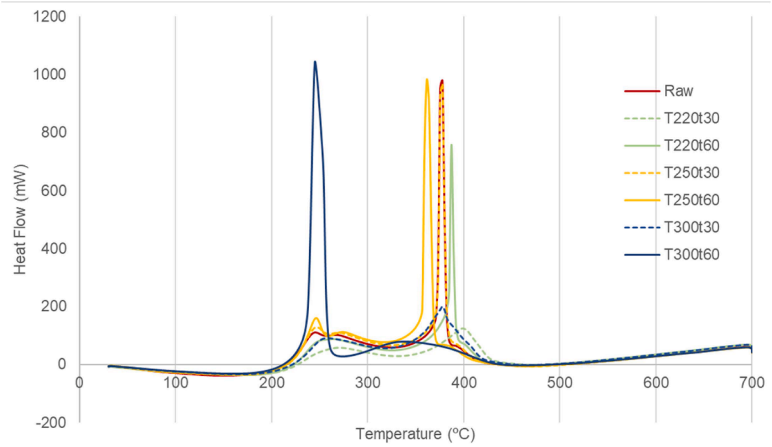

Fig. 2. DSC curves.

bounds and produce an exothermic reaction [78]. When addressing Fig. 1, no mass change was noted in the TGA curves at ~250 °C, however, the reactions responsible for the DSC peak such as surface oxidation or partial char combustion, might involve only a small fraction of the mass or be limited to superficial changes.

The fact that the exothermic peak is located at lower temperatures suggests that part of the energy required for the process can be internally supplied by the decomposition reactions themselves. This self-sustaining thermal behaviour can potentially reduce external energy input, making the process more energy-efficient. However, the potential risks associated with the enhanced reactivity of torrefied products must be addressed as the lower temperatures might indicate its propensity for spontaneous ignition during storage or transport. On the other hand, when addressing the remaining samples, as mentioned before, the peak is located at higher temperatures. While proteins and carbohydrates decomposition require high temperatures due to the complexity of the reaction, the more easily degradable molecules such as lipids and polysaccharides devolatilize at lower temperatures [61]. Between 200 °C and 400 °C the breakdown of C–C and C–H bonds in fatty acids and triglycerides together with the decomposition of cellulose produce exothermic reactions as can be seen in Fig. 2 [79].

Nevertheless, there are two samples that did not produce a significant peak during the DSC analysis: T220t30 and T300t30. In the first sample, this fact can be attributed to the less severe torrefaction conditions of the sample. At 220 °C and 30 min, the torrefaction severity is insufficient to trigger the extensive breakdown of hemicellulose, proteins, and lipids necessary to produce a well-defined main peak. On the other hand, for T300t30, the short residence time may allow partial volatilization of easily degradable components, such as proteins and lipids, but being insufficient for the accumulation of volatile release rates to form a distinct peak.

As mentioned before, the integration of DSC peak leads to a value that represents the exothermic reaction heat, which should be proportional to the HHV. These integral values are reported in Table 5 together with HHV estimations.

From these results it can be noticed that torrefaction increases reaction heat between 5 and 18%, and HHV up to 6%. The highest increases in both parameters were recorded for T300t60, (18% reaction heat and 6% HHV) reflecting the effectiveness of high-temperature and longer residence time conditions in enhancing energy properties.

Torrefaction increases reaction heat in every sample besides T220t60, which was slightly decreased if compared to raw sample. Although Fig. 2 shows some curves without the main peak, such as T220t30 and T300t30, it is possible to still integrate the curve and see that there is a constant exothermic reaction which releases almost a constant amount of heat from 200 °C to 400 °C. This phenomenon seems to take place when residence time is set at 30 min, besides sample T250t30, whose behaviour is very similar to the raw sample behaviour. In other words, when torrefaction process is applied using 30 min residence time, the molecule links are weakened enough to produce longer degradation exothermic reaction.

If HHV values are considered, the tendency shows that torrefaction increases HHV, as happened with the reaction heat. This result is consistent with the proximate analysis shown in Table 1, as fixed carbon content increased after torrefaction, and it is closely related to the high heating value and char formation [80]. However, torrefaction at 220 °C does not improve the energetic properties of the sewage sludge as HHV decreases. The same fact was noticed in the reaction heat for T220t60, but also, if T220t30 is considered, it can be noticed that it presents the lower reaction heat increase. However, it has to be taken into account the HHV values are estimated through proximate analysis and, therefore, discrepancies in the volatile matter, moisture and ash content values lead to discrepancies in the HHV. Besides the samples torrefied at 220 °C, sample T250t30 presents a lower HHV than the raw sample, but higher reaction heat. It seems that HHV value is not accurate enough in this case as, unlike reaction heat, decreases for T250t30. Nevertheless, sewage sludge inherent complexity in terms of composition introduces variability in thermal behaviour, particularly under conditions where reaction dynamics are sensitive to temperature and residence time. The consistent trends are only observed in three samples, a fact that highlights the critical influence of specific torrefaction parameters. These conditions result in more predictable thermal degradation pathways, which are important for optimizing the torrefaction process. However, further studies should consider calculating HHV using elemental analysis or calorimetry, in order to properly address the accuracy of the estimation.

Table 5
Reaction heat and HHV estimated values.

Sample	Reaction Heat (J/g)	HHV (MJ/kg)
Raw	5113.27	15.29
T220t30	5380.73	14.77
T220t60	4107.95	14.96
T250t30	5572.01	15.04
T250t60	5540.23	15.43
T300t30	6006.26	15.66
T300t60	6031.83	16.25

On the other hand, the highest reaction heat value was obtained for T300t60, which also lead to the highest HHV. This can be explained as the temperature and time are great enough to release most of the light volatiles and lead to a more energetic fuel. Indeed, TGA and DTG curves showed that the reaction when testing raw sewage sludge began to accelerate around 300 °C, therefore, when addressing T300t60 DTG curve it was noticed that the peak shifted to the right and decreased its maximum as the torrefaction process released the light volatiles.

Nevertheless, as previously pointed out by other authors, [81,82] the results seem to show that residence time presents a less significant influence on the energetic properties than torrefaction temperature, as both the reaction heat and the HHV estimated values do not present important deviations when addressing same temperature and different residence time.

3.3. Kinetic analysis

As mentioned in Section 2, kinetic analysis was performed using three different isoconversional methods: KAS, FWO and Friedman. Activation energy and preexponential factor was calculated for each method and for conversion degrees between 0.1 and 0.8 in order to avoid moisture release and char formation when addressing the reaction. Table 6 presents the average activation energy and preexponential factor values for each method and sample. Nevertheless, first test of T250t60 provided negative values, therefore, these data has not been considered when defining the average value.

Values obtained with all three methods are consistent. Slight differences can be found when comparing Friedman results with KAS and FWO mainly to the numerical instability associated with Friedman as it applies conversion rate data [83]. These differences increase when assessing preexponential factor, nevertheless, the same tendencies can be found in each method.

If the different samples are compared, it can be noticed that torrefaction reduces activation energy and preexponential factor values. Indeed, this decrease is greater when residence time is set at 30 min than when applying 60 min. Moreover, it can be noticed that torrefied samples present lower *Ea* values which means that the pyrolysis reaction is easier for torrefied samples. However, activation energy does not decrease when increasing torrefaction temperature, as when the sample is torrefied the molecular composition is modified, and the value depends on how the molecules change. Although several authors have focused on both sewage sludge torrefaction and sewage sludge pyrolysis kinetics, there is a lack of studies that focus on pyrolysis kinetics of torrefied sewage sludge samples. From the results presented in this study

Table 6
Pyrolysis activation energy and preexponential factor.

		KAS		FWO		Friedman	
	σ (%)	Ea (kJ/mol)	A (min^{-1})	Ea (kJ/mol)	A (min^{-1})	Ea (kJ/mol)	A (min^{-1})
Raw	1.77	344.45	6.28E+56	338.02	8.36E+54	375.43	2.18E+62
T220t30	1.85	253.96	2.15E+32	245.89	4.75E+31	252.90	7.53E+33
T220t60	1.78	300.70	4.97E+37	293.47	5.97E+36	298.61	6.02E+40
T250t30	2.44	260.94	1.25E+32	251.82	2.83E+31	260.28	4.23E+34
T250t60	1.83	320.68	5.60E+79	314.88	5.97E+76	356.19	3.07E+98
T300t30	1.77	271.02	8.14E+36	260.81	1.10E+36	270.32	5.74E+41
T300t60	2.43	305.24	1.15E+50	289.25	3.30E+48	299.72	3.92E+60

it is clear that torrefaction modifies the thermal degradation of the sample, a fact that has been previously noticed in other biomass samples [84], although the kinetic behaviour is related to the raw sample [85]. Indeed, Chen et al. [86], reported that torrefied rice biomass showed greater activation energies than the raw samples. Same tendency was found by Granados et al., when testing yellow poplar, but the opposite was found when analysing sugar cane bagasse [87]. Therefore, it seems that the increase or decrease of torrefied samples when compared to raw material might depend on the sample's composition.

Indeed, it has to be taken into account that sewage sludge composition significantly varies depending on the sample, therefore, the activation energy might change from one sample to another. Naqvi et al. [39], compiled information from several studies, finding out that previously reported activation energies for sewage sludge kinetics might vary from ~5 kJ/mol up to more than 500 kJ/mol. Nevertheless, the results seem to be consistent with previously published literature. Scott et al. [36] reported activation energy values up to 350 kJ/mol for sewage sludge using an iterative algorithm, while Liu et al. [88] reported values up to 560 kJ/mol using model free methods. Similar values were reported by Wielinski et al. [89], however considering a combustion process.

If *Ea* values are plotted versus conversion degree, it is possible to see how activation energy varies as the reaction progresses. Fig. 3 plots these curves for each sample and method. Similar tendencies can be seen in samples torrefied for 30 min, especially if T220t30 and T250t30 samples are considered.

Indeed, almost every sample presents the same tendency increasing *Ea* when α increases as already noticed by Gasparovic et al. [32,90], besides raw and T300t60 samples. Raw sample presents slight variations at the beginning of the reaction, probably due to moisture release, which is significantly higher in this sample than in the torrefied ones. Samples activation energies reach their maximum at the highest conversion degree besides T300t60, which presents almost a steady curve with constant *Ea* values until α reaches 0.7, when activation energy presents a peak and afterward heavily decreases even to negative values. This can be explained due to the fact that the sample presents the most severe torrefaction process and therefore, the volatile matter has been mostly released leading to a steadier pyrolysis reaction.

3.4. Thermodynamic analysis

Figs. 4-6 presents the results obtained from the thermodynamic analysis, where ΔH, ΔG, and ΔS curves are graphed for each level of conversion and for each kinetic method.

The mean value of the enthalpy (ΔH) follows a similar trend to the activation energy [45]. The difference between both parameters ranges from 5.23 to 5.69 kJ/mol, with the minimum value assigned to the untreated sample and the maximum value to the torrefied sample at a higher temperature and time (T300t60). These results can be explained due to the fact that the torrefied samples have undergone more changes during the reaction, leading to greater discrepancies between the parameters. As shown in Fig. 4, the enthalpy values calculated for the raw sample according to Friedman, KAS, and FWO are 337.23 kJ/mol, 329.70 kJ/mol, and 375.26 kJ/mol, respectively. In contrast, the torrefied samples range from 242.12 to 351.47 kJ/mol. The obtained values agree with the studies conducted by previous authors [91]. According to the technical analysis, it is evident that the raw sample requires less thermal energy for bond dissociation compared to the torrefied samples.

Furthermore, the Gibbs free energy (ΔG) represents the total rise in energy within the system while the activated complex forms, providing insights into the bioenergy capacity of the biomass. Moreover, Gibbs free energy is a clear indicator of the spontaneity of a reaction. The values of the Gibbs free energy for the untreated sample fall within the range of 254.12 to 279.45 kJ/mol, close to those reported by Petrovič et al., 2021 [91]. Similar values are obtained for the torrefied samples especially for samples torrefied for 60 min residence time. Given that both enthalpy variation and Gibbs free energy are positive, it confirms that the process is non-spontaneous and involves the input of thermal energy.

When assessing entropy values (ΔS), it has to be noted that entropy denotes the level of disorder present in a system reaction process. A low magnitude suggests that the process is nearing equilibrium. Conversely, high reactivity implies that the process will proceed more rapidly to form the activated complex, necessitating shorter operation times. In essence, as the entropy value increases, so does the reactivity of the system. As depicted in Fig. 6, entropy values tend to rise as the degree of reaction increases. Again, 60 min residence time lead to higher entropy values, although no torrefied sample reaches the values obtained when addressing raw sample. Specifically the raw sample, values range between 0.126–0.161 kJ/mol·K, in contrast to the torrefied samples, varying from 0.1061 to 0.139 kJ/mol·K.

3.5. Self-ignition risk

As mentioned before, self-ignition or self-heating risk was addressed using two different procedures. Fig. 7 shows the results obtained when applying García-Torrent et al. methodology [53]. It can be noticed that almost every sample presented a low self-ignition risk besides the samples submitted to 300 °C torrefaction. Again, from these results it can be noticed that the residence time does not influence self-ignition as much as torrefaction temperature.

All the samples present similar activation energies, between 70 and 80 kJ/mol. Note that these values are completely different to those presented in Table 6. As mentioned before, for kinetic analysis model free methods were used, while Fig. 7 uses activation energy calculated assuming a first order reaction (Cumming's equation). Furthermore, differences between activation energy values are not only due to the kinetic model but also to the simulated process, as the results reported in Table 6 correspond to a pyrolysis reaction, while Fig. 7 activation energy corresponds to samples combustion.

Therefore, if all the samples present the same activation energy range, the different classification is produced due to T_{char}. Indeed, T300t30 and T300t60 samples showed a significantly lower T_{char} than the remaining samples. This fact can be related to the results observed in Fig. 2, as T300t60 sample fasten the reaction before 300 °C. It can be concluded that, samples torrefied at 300 °C present more oxygen

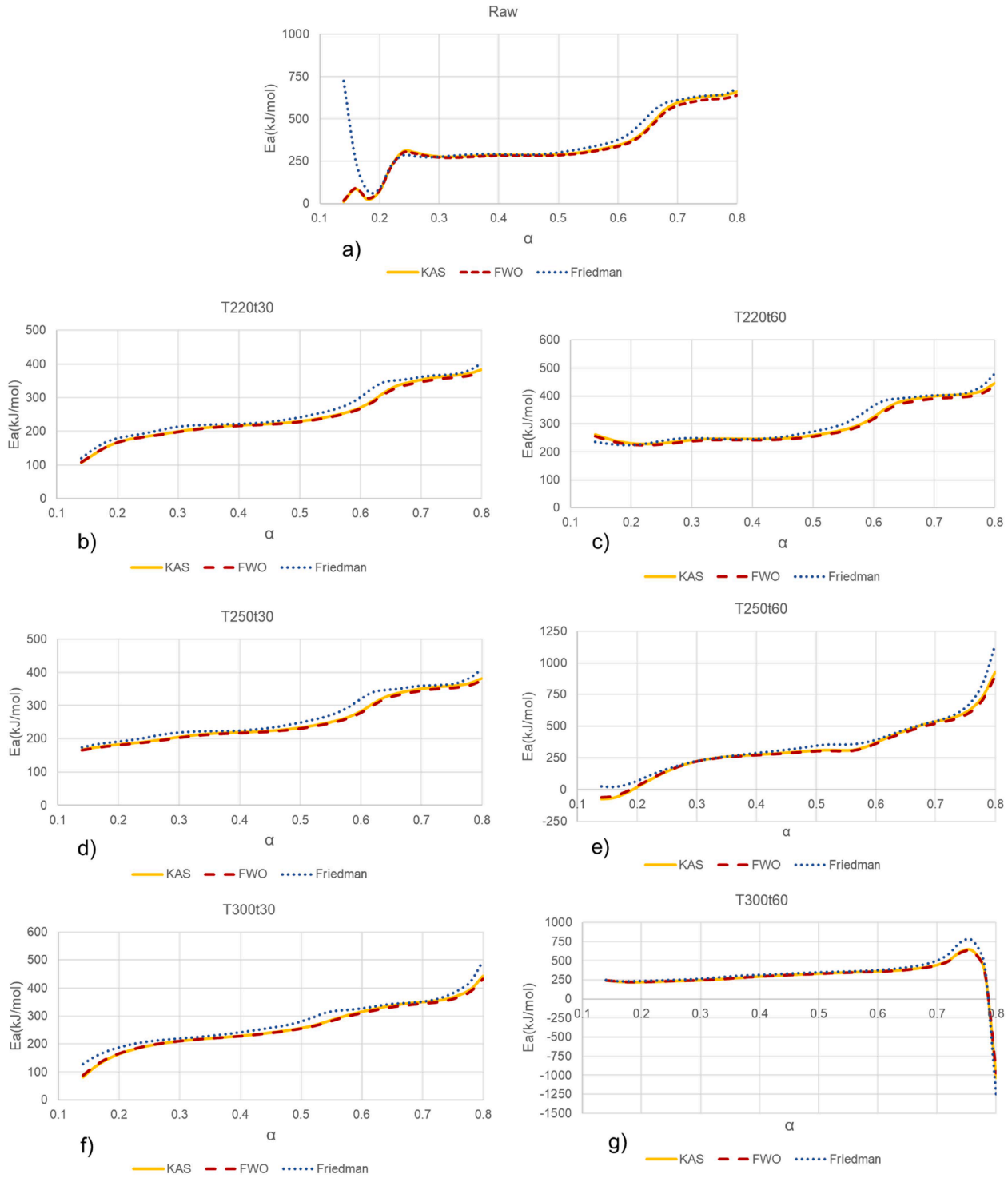

Fig. 3. Activation energy curves for each kinetic method and sample: raw (a), T220t30 (b), T220t60 (c), T250t30 (d), T250t60 (e), T300t30 (f) and T300y60 (g).

reactivity and therefore, the oxidation takes place at lower temperatures resulting into a classification of high self-ignition risk. This fact was also noticed when addressing the reaction heat and the HHV, as the increase noted in these parameters for samples torrefied at 300 °C indicates a greater energy release during oxidation, enhanced reactivity from a porous structure, and the presence of residual volatiles. These factors amplify heat generation, which, if not dissipated effectively, can lead to temperature buildup and spontaneous ignition during storage.

If the results obtained are compared to previously published literature it has to be noted that important differences in the self-ignition risk depending on the composition can be found, as pointed out by Díaz et al. [92]. Indeed, usually biomasses present a higher self-ignition risk, with a classification between medium and high risk [93], among which sewage sludge often presents a high self-ignition risk [53] although it depends on the volatile content and the HHV.

Nevertheless, it has to be noted that, although when applying oxygen atmosphere usually the mass drops producing almost a vertical line in the TGA curves and only ashes remain, when sewage sludge samples are addressed sometimes this phenomenon is not observed, and the mass drop is progressive. In those cases, T_{char} actually corresponds to the

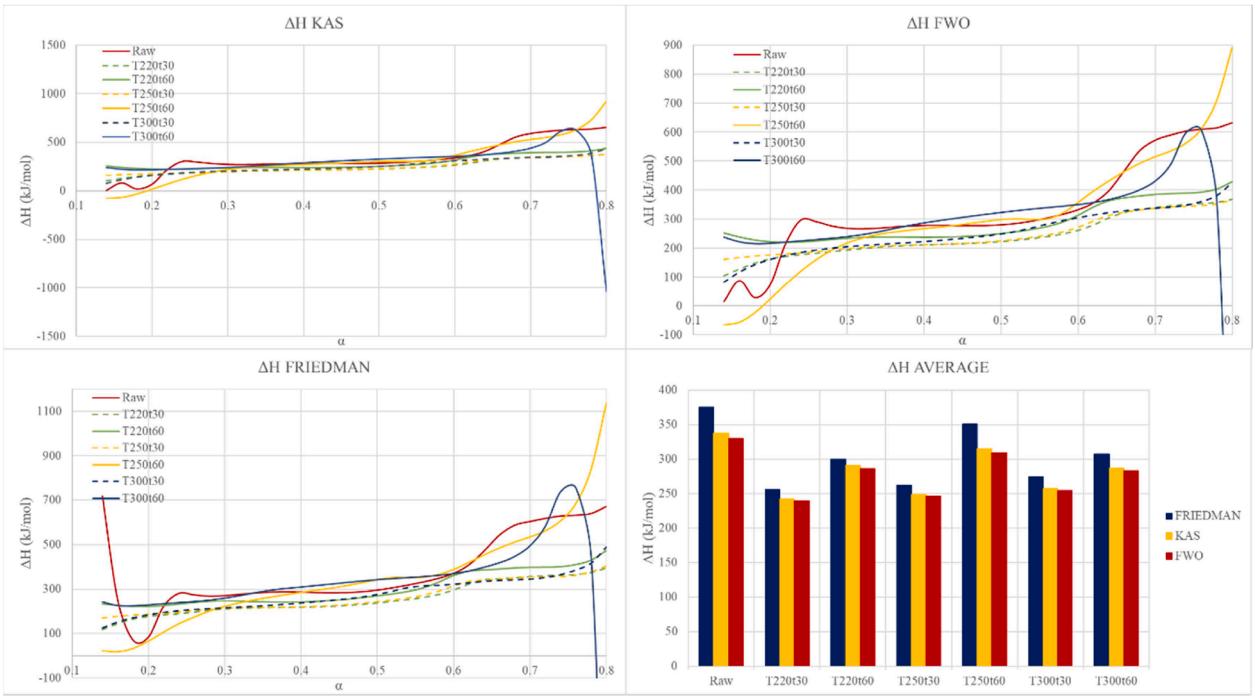

Fig. 4. Enthalpy change curves for each kinetic method and sample.

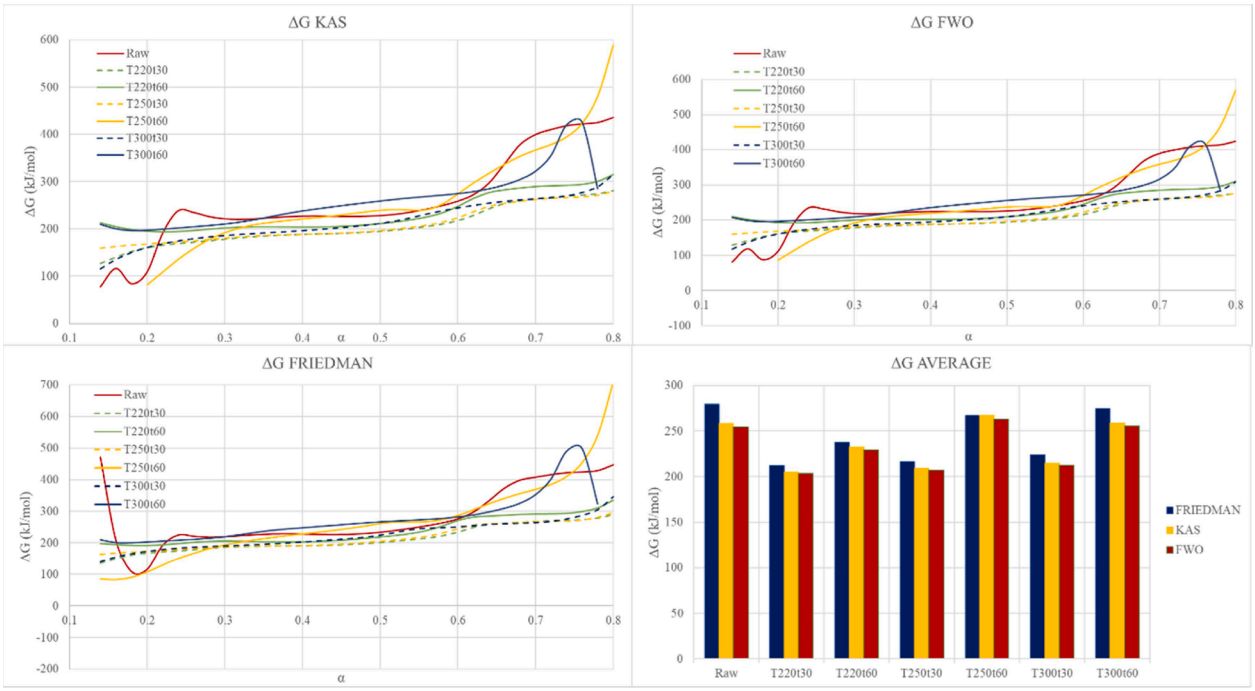

Fig. 5. Gibbs free energy change curves for each kinetic method and sample.

temperature at which the oxidation accelerates, and the reaction fastens, which is the present case. This fact can be explained due to sewage sludge composition, as light volatiles and heavy volatiles release takes place in separated stages as it was noticed in Fig. 1.

If the second method proposed by Jankovic et al. [56] is considered, similar tendencies are found. Table 7 shows the microscopic devolatilization rate (ψ) values obtained for each sample and heating rate together with the average values.

Microscopic devolatilization rate is related to devolatilization mechanism of coals and, as can be noticed from its definition in Eq. (4), it depends on the volatile content. Once microscopic devolatilization rate is obtained, it is possible to address the slope factor in order to obtain TG_{spi}. Fig. 8 represents reference temperatures versus *coef* average values for each point (peak start, inflection, and peak end) and sample.

Therefore, from this data it is possible to calculate the slope necessary to determine TG_{spi} as the figure also plots the straight line whose slope will be used to define TG_{spi}. Table 8 reports TG_{spi} values together with spontaneous ignition potential classification.

Although every assessed sample is classified as "Non-reactive", if

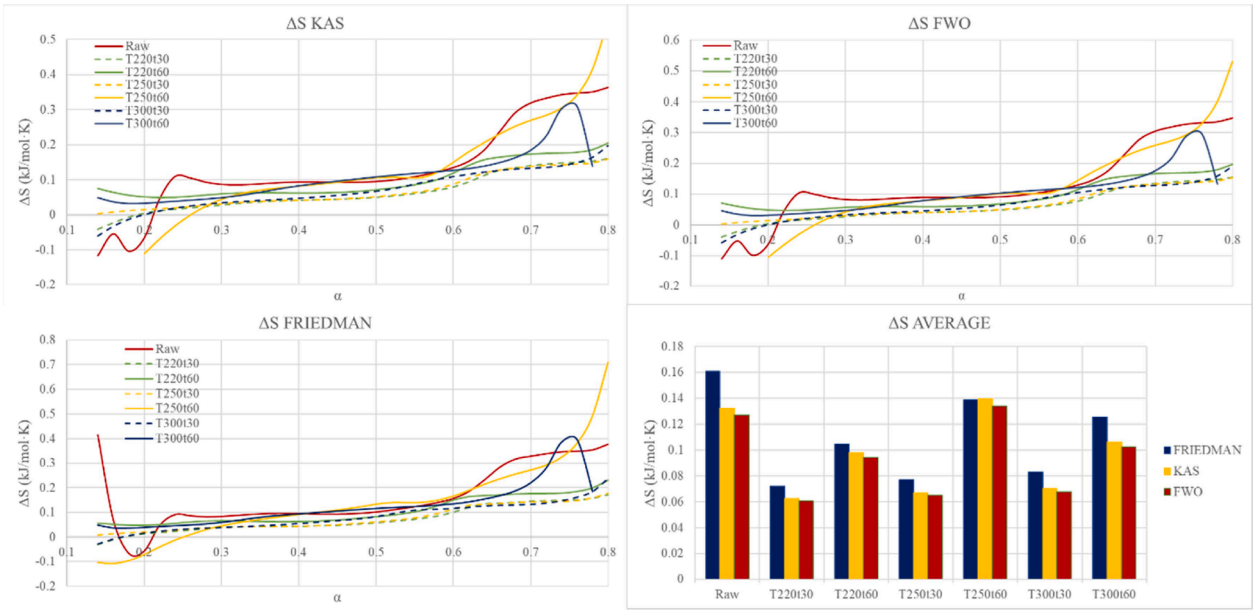

Fig. 6. Entropy change curves for each kinetic method and sample.

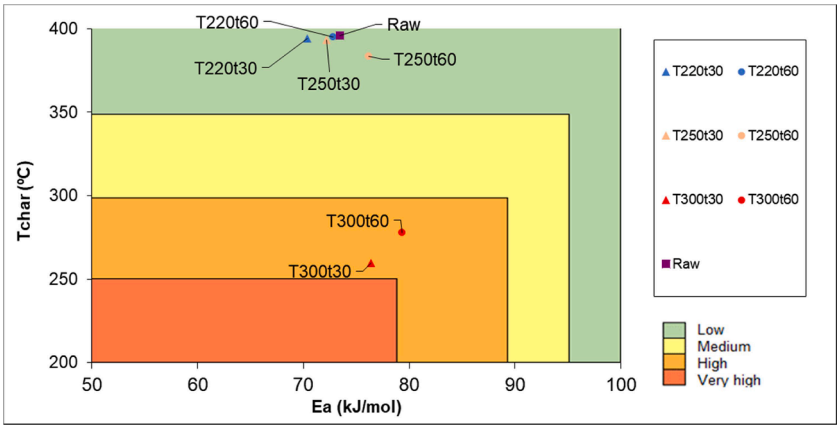

Fig. 7. Self-ignition risk classification.

Table 7
Microscopic devolatilization rate values.

Ψ (% · min $^{-1}$)	β 3 K/min	β 5 K/min	β 7 K/min	β 10 K/min	β 20 K/min	Mean
Raw	0.4991	0.7811	0.8665	1.2211	2.9936	1.2723
T220t30	0.4670	0.7514	1.0415	1.4611	2.8066	1.3055
T220t60	0.3856	0.7481	0.8600	1.5099	2.4371	1.1881
T250t30	0.5089	0.8296	1.3614	1.6061	3.1645	1.4941
T250t60	0.4675	0.7522	1.1716	1.4787	2.8486	1.3437
T300t30	0.4799	0.9182	1.0555	1.5710	2.9146	1.3878
T300t60	0.3939	0.5200	0.7033	0.9912	2.4298	1.0076

TG_{spi} values are addressed important differences can be noticed. Torrefaction significantly increases TG_{spi} index, besides sample T300t60, therefore, it is clear that the remark previously mentioned: torrefaction presents an effect on the self-ignition risk that should be considered. Moreover, it was found that samples torrefied at 60 min residence time led to lower TG_{spi} values than samples torrefied at 30 min residence time, besides T220t60. Nevertheless, there are no significant differences between samples regarding TG_{spi} index, therefore, the influence of torrefaction temperature or residence time seems to be negligible when addressing TG_{spi}.

Differences between both methods can be observed. This can be partly explained due to the fact that the method proposed by Jankovic et al. [56] is designed for coals and has not been used in biomasses, indeed, it was already pointed out in a previous study that the use of this method might lead to inaccurate results [94]. Moreover, these methods rely on different principals which also add variations in the self-ignition risk prediction. The implementation of more than one heating rate in the self-ignition risk classification might lead to more accurate results and address thermal phenomenon that now are not considered. Nevertheless, it has proved to provide important information regarding the behaviour of the samples.

4. Conclusions

This study analyzed torrefied sewage sludge using several thermogravimetric analysis (TGA) methods, addressing thermal behavior from energy and autoignition risk perspectives. The results show that torrefaction offers several benefits for sewage sludge management, significantly reducing moisture content and increasing calorific value (HHV), making it a more attractive fuel source for energy recovery.

The torrefaction temperature has a greater impact on HHV and heat

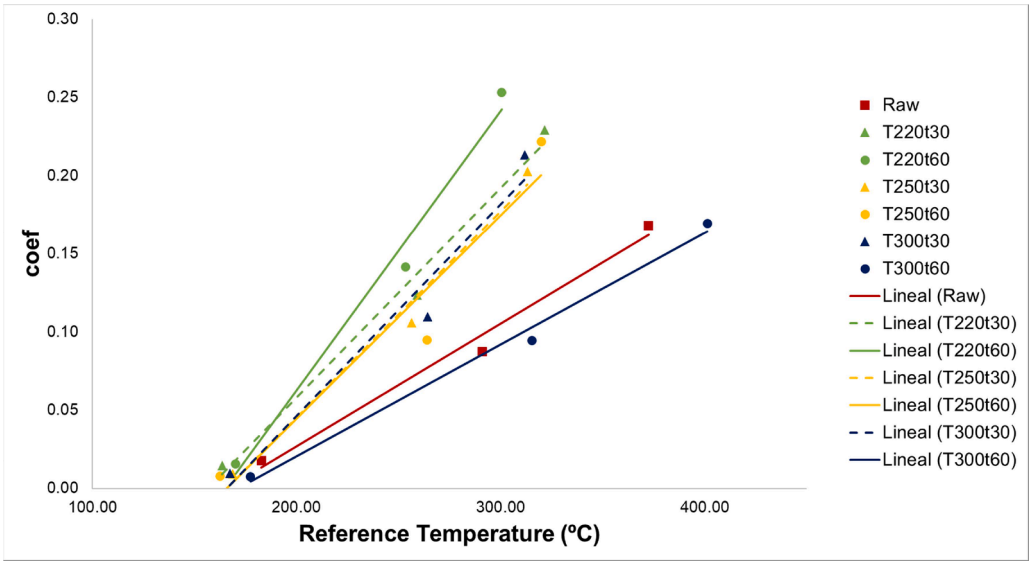

Fig. 8. Linear relationship between *coef* values and reference temperatures for each sample.

Table 8
TG_{spi} index values and classification.

	TG_{spi} (%· °C^{-1}·min^{-1})	Classification
Raw	0.0010	Non-reactive
T220t30	0.0017	Non-reactive
T220t60	0.0021	Non-reactive
T250t30	0.0019	Non-reactive
T250t60	0.0017	Non-reactive
T300t30	0.0019	Non-reactive
T300t60	0.0007	Non-reactive

of reaction than residence time. Sample T300t60, torrefied at 300 °C for 60 min, presented the highest values of HHV and heat of reaction. Although HHV data for some torrefied samples were lower than those of the raw sample, heat of reaction values were consistent, demonstrating the improvements of torrefaction. Future studies should obtain accurate HHVs to validate these estimates.

In the pyrolysis kinetic analysis, torrefied samples showed a lower activation energy than the raw sample, especially with 30 min of residence time. This suggests a significant relationship between torrefaction parameters and pyrolysis activation energy. The activation energy increased with the degree of conversion, indicating that higher thermal decomposition requires more energy. Sample T300t60 showed a constant evolution of Ea values up to a degree of conversion of 0.7, when Ea increased slightly and then decreased to negative values, indicating significant changes in the molecular structure.

Finally, torrefaction influences the autoignition tendency of sewage sludge. Samples torrefied at 300 °C were classified as having a high autoignition risk due to their higher reactivity to oxygen. This study is the first to apply dual methodologies to assess the autoignition risk in torrefied sewage sludge, highlighting an increased risk correlated with higher calorific values. Nevertheless, further research should consider improving these methods by increasing the number of heating rates or modifying the devolatilization to fit biomass combustion. Also, it could be interesting to implement different methods to define self-ignition risk that do not rely on the thermogravimetric analysis, in order to improve the understanding. In conclusion, sewage sludge torrefaction is a promising technology for waste management, offering significant benefits for energy recovery and soil amendment, although it is crucial to consider the associated ignition risk.

CRediT authorship contribution statement

Blanca Castells: Conceptualization, Methodology, Validation, Investigation, Writing – original draft. **Roberto Paredes:** Conceptualization, Software, Methodology, Writing – original draft. **David León:** Software, Investigation, Writing – original draft. **Isabel Amez:** Validation, Investigation, Writing – review & editing.

Declaration of competing interest

The authors declare that they have no known competing financial interests or personal relationships that could have appeared to influence the work reported in this paper.

Data availability

No data was used for the research described in the article.

References

[1] Z. Wang, Q. Bui, B. Zhang, T.L.H. Pham, Biomass energy production and its impacts on the ecological footprint: an investigation of the G7 countries, Sci. Total Environ. 743 (2020) 140741, https://doi.org/10.1016/j.scitotenv.2020.140741.
[2] S.J. Ergun, P.A. Owusu, M.F. Rivas, Determinants of renewable energy consumption in Africa, Environ. Sci. Pollut. Res. 26 (2019) 15390–15405, https://doi.org/10.1007/s11356-019-04567-7.
[3] C.B. Field, J.E. Campbell, D.B. Lobell, Biomass energy: the scale of the potential resource, Trends Ecol. Evol. 23 (2008) 65–72, https://doi.org/10.1016/j.tree.2007.12.001.
[4] S.V. Vassilev, D. Baxter, L.K. Andersen, C.G. Vassileva, An overview of the chemical composition of biomass, Fuel 89 (2010) 913–933.
[5] F. Bilgili, E. Koçak, Ü. Bulut, S. Kuşkaya, Can biomass energy be an efficient policy tool for sustainable development? Renew. Sustain. Energy Rev. 71 (2017) 830–845, https://doi.org/10.1016/j.rser.2016.12.109.
[6] P. McKendry, Energy production from biomass (part 1): overview of biomass, Bioresour. Technol. 83 (2002) 37–46, https://doi.org/10.1016/S0960-8524(01)00118-3.
[7] R. Vakulchuk, I. Overland, D. Scholten, Renewable energy and geopolitics: a review, Renew. Sustain. Energy Rev. 122 (2020) 109547, https://doi.org/10.1016/j.rser.2019.109547.
[8] M.E. Arce, Á. Saavedra, J.L. Míguez, E. Granada, A. Cacabelos, Biomass fuel and combustion conditions selection in a fixed bed combustor, Energies 6 (2013) 5973–5989, https://doi.org/10.3390/en6115973.
[9] C.S. Liew, N.M. Yunus, B.S. Chidi, M.K. Lam, P.S. Goh, M. Mohamad, J.C. Sin, S. M. Lam, J.W. Lim, S.S. Lam, A review on recent disposal of hazardous sewage sludge via anaerobic digestion and novel composting, J. Hazard. Mater. 423 (2022) 126995.
[10] N. Gao, K. Kamran, C. Quan, P.T. Williams, Thermochemical conversion of sewage sludge: a critical review, Prog. Energy Combust. Sci. 79 (2020) 100843, https://doi.org/10.1016/j.pecs.2020.100843.

[11] J.S. Tumuluru, S. Sokhansanj, J.R. Hess, C.T. Wright, R.D. Boardman, A review on biomass torrefaction process and product properties for energy applications, Ind. Biotechnol. 7 (2011) 384–401, https://doi.org/10.1089/ind.2011.7.384.
[12] J. Pulka, P. Manczarski, J.A. Koziel, A. Białowiec, Torrefaction of sewage sludge: kinetics and fuel properties of biochars, Energies 12 (2019), https://doi.org/10.3390/en12030565.
[13] M. Atienza-Martínez, I. Fonts, J. Ábrego, J. Ceamanos, G. Gea, Sewage sludge torrefaction in a fluidized bed reactor, Chem. Eng. J. 222 (2013) 534–545, https://doi.org/10.1016/j.cej.2013.02.075.
[14] J. Poudel, T.-I. Ohm, S.-H. Lee, S.C. Oh, A study on torrefaction of sewage sludge to enhance solid fuel qualities, Waste Manag. 40 (2015) 112–118, https://doi.org/10.1016/j.wasman.2015.03.012.
[15] K.M. Haider, F. Lafouge, Y. Carpentier, S. Houot, D. Petitprez, B. Loubet, C. Focsa, R. Ciuraru, Chemical identification and quantification of volatile organic compounds emitted by sewage sludge, Sci. Total Environ. 838 (2022) 155948, https://doi.org/10.1016/j.scitotenv.2022.155948.
[16] C. Nobre, O. Alves, A. Longo, C. Vilarinho, M. Gonçalves, Torrefaction and carbonization of refuse derived fuel: char characterization and evaluation of gaseous and liquid emissions, Bioresour. Technol. 285 (2019) 121325, https://doi.org/10.1016/j.biortech.2019.121325.
[17] M. Atienza-Martínez, I. Fonts, L. Lázaro, J. Ceamanos, G. Gea, Fast pyrolysis of torrefied sewage sludge in a fluidized bed reactor, Chem. Eng. J. 259 (2015) 467–480, https://doi.org/10.1016/j.cej.2014.08.004.
[18] P. Piersa, S. Szufa, J. Czerwińska, H. Ünyay, Ł. Adrian, G. Wielgosinski, A. Obraniak, W. Lewandowska, M. Marczak-Grzesik, M. Dzikuć, Pine Wood and Sewage Sludge Torrefaction Process for Production Renewable Solid Biofuels and Biochar as Carbon Carrier for Fertilizers, Energies 14 (2021) 8176.
[19] A.B. Hernández, F. Okonta, N. Freeman, Sewage sludge charcoal production by N2- and CO2-torrefaction, J. Environ. Chem. Eng. 5 (2017) 4406–4414.
[20] E. Agrafioti, G. Bouras, D. Kalderis, E. Diamadopoulos, Biochar production by sewage sludge pyrolysis, J. Anal. Appl. Pyrolysis. 101 (2013) 72–78.
[21] A. Gopinath, G. Divyapriya, V. Srivastava, A.R. Laiju, P.V. Nidheesh, M.S. Kumar, Conversion of sewage sludge into biochar: a potential resource in water and wastewater treatment, Environ. Res. 194 (2021) 110656.
[22] P. Elbl, T. Sitek, J. Lachman, M. Lisý, M. Baláš, J. Pospíšil, Sewage sludge and wood sawdust co-firing: gaseous emissions and particulate matter size distribution, Energy 256 (2022) 124680, https://doi.org/10.1016/j.energy.2022.124680.
[23] A. Zhou, X. Wang, A. Magdziarz, S. Yu, S. Deng, J. Bai, Q. Zhang, H. Tan, Ash fusion and mineral evolution during the co-firing of coal and municipal sewage sludge in power plants, Fuel 310 (2022) 122416, https://doi.org/10.1016/j.fuel.2021.122416.
[24] P. Trop, M. Agrez, D. Urbancl, D. Goricanec, Co-gasification of torrefied wood biomass and sewage sludge, in: Z. Kravanja, M.B.T.-C.A.C.E. Bogataj (Eds.), 26 Eur. Symp. Comput. Aided Process Eng, Elsevier, 2016, pp. 2229–2234, https://doi.org/10.1016/B978-0-444-63428-3.50376-3.
[25] K. Głód, J.A. Lasek, K. Supernok, P. Pawłowski, R. Fryza, J. Zuwała, Torrefaction as a way to increase the waste energy potential, Energy 285 (2023) 128606, https://doi.org/10.1016/j.energy.2023.128606.
[26] A. Petrovič, J. Stergar, L. Škodič, N. Rašl, T. Cenčič Predikaka, L. Čuček, D. Goričanec, D. Urbancl, Thermo-kinetic analysis of pyrolysis of thermally pre-treated sewage sludge from the food industry, Therm. Sci. Eng. Prog. 42 (2023) 101863, https://doi.org/10.1016/j.tsep.2023.101863.
[27] A. Magdziarz, M. Wilk, Thermogravimetric study of biomass, sewage sludge and coal combustion, Energy Convers. Manag. 75 (2013) 425–430, https://doi.org/10.1016/j.enconman.2013.06.016.
[28] A. Magdziarz, S. Werle, Analysis of the combustion and pyrolysis of dried sewage sludge by TGA and MS, Waste Manag. 34 (2014) 174–179, https://doi.org/10.1016/j.wasman.2013.10.033.
[29] D.L. Urban, M.J. Antal Jr, Study of the kinetics of sewage sludge pyrolysis using DSC and TGA, Fuel 61 (1982) 799–806.
[30] J. de Oliveira Silva, G. Rodrigues Filho, C. da Silva Meireles, S.D. Ribeiro, J. G. Vieira, C.V. da Silva, D.A. Cerqueira, Thermal analysis and FTIR studies of sewage sludge produced in treatment plants. The case of sludge in the city of Uberlândia-MG, Brazil, Thermochim. Acta. 528 (2012) 72–75.
[31] E. Smidt, J. Tintner, Application of differential scanning calorimetry (DSC) to evaluate the quality of compost organic matter, Thermochim. Acta. 459 (2007) 87–93.
[32] Y.W. Huang, M.Q. Chen, H.F. Luo, Nonisothermal torrefaction kinetics of sewage sludge using the simplified distributed activation energy model, Chem. Eng. J. 298 (2016) 154–161.
[33] Q. Nguyen, D.D. Nguyen, H. Vothi, C. He, M. Goodarzi, Q.-V. Bach, Isothermal torrefaction kinetics for sewage sludge pretreatment, Fuel 277 (2020) 118103.
[34] J. Shao, R. Yan, H. Chen, B. Wang, D.H. Lee, D.T. Liang, Pyrolysis characteristics and kinetics of sewage sludge by thermogravimetry fourier transform infrared analysis, Energy Fuels 22 (2008) 38–45, https://doi.org/10.1021/ef700287p.
[35] Y. Zhai, W. Peng, G. Zeng, Z. Fu, Y. Lan, H. Chen, C. Wang, X. Fan, Pyrolysis characteristics and kinetics of sewage sludge for different sizes and heating rates, J. Therm. Anal. Calorim. J Therm Anal Calorim. 107 (2012) 1015–1022, https://doi.org/10.1007/s10973-011-1644-0.
[36] S.A. Scott, J.S. Dennis, J.F. Davidson, A.N. Hayhurst, Thermogravimetric measurements of the kinetics of pyrolysis of dried sewage sludge, Fuel 85 (2006) 1248–1253, https://doi.org/10.1016/j.fuel.2005.11.003.
[37] J. Gong, L. Yang, A review on flaming ignition of solid combustibles: pyrolysis kinetics, experimental methods and modelling, Fire Technol. 60 (2024) 893–990, https://doi.org/10.1007/s10694-022-01339-7.
[38] O. Senneca, F. Cerciello, Kinetics of combustion of lignocellulosic biomass: recent research and critical issues, Fuel 347 (2023) 128310, https://doi.org/10.1016/j.fuel.2023.128310.
[39] S.R. Naqvi, R. Tariq, M. Shahbaz, M. Naqvi, M. Aslam, Z. Khan, H. Mackey, G. Mckay, T. Al-Ansari, Recent developments on sewage sludge pyrolysis and its kinetics: resources recovery, thermogravimetric platforms, and innovative prospects, Comput. Chem. Eng. 150 (2021) 107325, https://doi.org/10.1016/j.compchemeng.2021.107325.
[40] S. Vikram, P. Rosha, S. Kumar, Recent modeling approaches to biomass pyrolysis: a review, Energy Fuels 35 (2021) 7406–7433, https://doi.org/10.1021/acs.energyfuels.1c00251.
[41] R. Chen, Q. Li, X. Xu, D. Zhang, R. Hao, Combustion characteristics, kinetics and thermodynamics of Pinus Sylvestris pine needle via non-isothermal thermogravimetry coupled with model-free and model-fitting methods, Case Stud, Therm. Eng. 22 (2020) 100756, https://doi.org/10.1016/j.csite.2020.100756.
[42] Z. Zhang, H. Duan, Y. Zhang, X. Guo, X. Yu, X. Zhang, M.M. Rahman, J. Cai, Investigation of kinetic compensation effect in lignocellulosic biomass torrefaction: kinetic and thermodynamic analyses, Energy 207 (2020), https://doi.org/10.1016/j.energy.2020.118290.
[43] S.R. Naqvi, R. Tariq, Z. Hameed, I. Ali, S.A. Taqvi, M. Naqvi, M.B.K. Niazi, T. Noor, W. Farooq, Pyrolysis of high-ash sewage sludge: thermo-kinetic study using TGA and artificial neural networks, Fuel 233 (2018) 529–538, https://doi.org/10.1016/j.fuel.2018.06.089.
[44] B. Gajera, U. Tyagi, A.K. Sarma, M.K. Jha, Impact of torrefaction on thermal behavior of wheat straw and groundnut stalk biomass: kinetic and thermodynamic study, Fuel Commun. 12 (2022) 100073, https://doi.org/10.1016/j.jfueco.2022.100073.
[45] M. Ivanovski, A. Petrovic, I. Ban, D. Goricanec, D. Urbancl, Determination of the kinetics and thermodynamic parameters of lignocellulosic biomass subjected to the torrefaction process, Materials (Basel) 14 (2021), https://doi.org/10.3390/ma14247877.
[46] A. Białowiec, J. Pulka, M. Styczyńska, J.A. Koziel, J. Kalka, M. Jureczko, E. Felis, P. Manczarski, Is Biochar from the Torrefaction of Sewage Sludge Hazardous Waste? Materials (Basel) 13 (2020) https://doi.org/10.3390/ma13163544.
[47] B. Castells, I. Amez, L. Medic, N. Fernandez-Anez, J. Garcia-Torrent, Study of lignocellulosic biomass ignition properties estimation from thermogravimetric analysis, J. Loss Prev. Process Ind. (2021) 104425, https://doi.org/10.1016/j.jlp.2021.104425.
[48] B. Batidzirai, A.P.R. Mignot, W.B. Schakel, H.M. Junginger, A.P.C. Faaij, Biomass torrefaction technology: techno-economic status and future prospects, Energy 62 (2013) 196–214, https://doi.org/10.1016/j.energy.2013.09.035.
[49] E. Arriola, W.-H. Chen, Y.-K. Chih, M.D. De Luna, P.L. Show, Impact of post-torrefaction process on biochar formation from wood pellets and self-heating phenomena for production safety, Energy 207 (2020) 118324, https://doi.org/10.1016/j.energy.2020.118324.
[50] E. Menya, C. Okello, H. Storz, J. Wakatuntu, M. Turyasingura, D.K. Okot, S. Kizito, A.J. Komakech, I. Kabenge, S. Rwahwire, P.W. Olupot, A review of progress on torrefaction, pyrolysis and briquetting of banana plant wastes for biofuels, Biomass Convers. Biorefinery. (2024), https://doi.org/10.1007/s13399-024-06204-x.
[51] P.N.Y. Yek, Y.W. Cheng, R.K. Liew, W.A. Wan Mahari, H.C. Ong, W.H. Chen, W. Peng, Y.K. Park, C. Sonne, S.H. Kong, M. Tabatabaei, M. Aghbashlo, S.S. Lam, Progress in the torrefaction technology for upgrading oil palm wastes to energy-dense biochar: a review, Renew. Sustain. Energy Rev. 151 (2021) 111645, https://doi.org/10.1016/J.RSER.2021.111645.
[52] R. Bertani, A. Biasin, P. Canu, M. Della Zassa, D. Refosco, F. Simionato, M. Zerlottin, Self-heating of dried industrial tannery wastewater sludge induced by pyrophoric iron sulfides formation, J. Hazard. Mater. 305 (2016) 105–114, https://doi.org/10.1016/j.jhazmat.2015.11.038.
[53] J. Garcia-Torrent, Á. Ramírez, N. Fernandez-Anez, L. Medic, A. Tascón, Influence of the composition of solid biomass in the flammability and susceptibility to spontaneous combustion, Fuel 184 (2016) 503–511, https://doi.org/10.1016/j.fuel.2016.07.045.
[54] M. Simonic, D. Goricanec, D. Urbancl, Impact of torrefaction on biomass properties depending on temperature and operation time, Sci. Total Environ. 740 (2020) 140086, https://doi.org/10.1016/J.SCITOTENV.2020.140086.
[55] R. Ahmad, A... Ahmad, S... Mohammed, W.A... Wan Ahmad, V. Vijean, R. Santiagoo, N... Ibrahim, N. Udin, Influence of Torrefaction on Sewage Sludge, IOP Conf. Ser. Earth Environ, Sci. 1135 (2023) 012036, https://doi.org/10.1088/1755-1315/1135/1/012036.
[56] B. Janković, N.G. Manić, D.D. Stojiljković, V.V. Jovanović, The assessment of spontaneous ignition potential of coals using TGA–DTG technique, Combust. Flame. 211 (2020) 32–43, https://doi.org/10.1016/j.combustflame.2019.09.020.
[57] D. Losic, F. Farivar, P.L. Yap, Refining and Validating Thermogravimetric Analysis (TGA) for Robust Characterization and Quality Assurance of Graphene-Related Two-Dimensional Materials (GR2Ms), C 10 (2024), https://doi.org/10.3390/c10020030.
[58] K.M. Czajka, The impact of the thermal lag on the interpretation of cellulose pyrolysis, Energy 236 (2021) 121497, https://doi.org/10.1016/j.energy.2021.121497.
[59] I. Estiati, F.B. Freire, J.T. Freire, R. Aguado, M. Olazar, Fitting performance of artificial neural networks and empirical correlations to estimate higher heating values of biomass, Fuel 180 (2016) 377–383, https://doi.org/10.1016/J.FUEL.2016.04.051.
[60] S. Hosseinpour, M. Aghbashlo, M. Tabatabaei, M. Mehrpooya, Estimation of biomass higher heating value (HHV) based on the proximate analysis by using

iterative neural network-adapted partial least squares (INNPLS), Energy 138 (2017) 473–479, https://doi.org/10.1016/j.energy.2017.07.075.
[61] N. Miskolczi, S. Tomasek, Investigation of Pyrolysis Behavior of Sewage Sludge by Thermogravimetric Analysis Coupled with Fourier Transform Infrared Spectrometry Using Different Heating Rates, Energies 15 (2022), https://doi.org/10.3390/en15145116.
[62] S. Vyazovkin, A.K. Burnham, J.M. Criado, L.A. Pérez-Maqueda, C. Popescu, N. Sbirrazzuoli, ICTAC Kinetics Committee recommendations for performing kinetic computations on thermal analysis data, Thermochim. Acta. 520 (2011) 1–19, https://doi.org/10.1016/j.tca.2011.03.034.
[63] H.L. Friedman, Kinetics of thermal degradation of char-forming plastics from thermogravimetry. Application to a phenolic plastic, J. Polym. Sci. Part C Polym. Symp. 6 (1964) 183–195, https://doi.org/10.1002/polc.5070060121.
[64] H.E. Kissinger, Reaction Kinetics in Differential Thermal Analysis, Anal. Chem 29 (1957) 1702–1706, https://doi.org/10.1021/ac60131a045.
[65] T. Akahira, T. Sunose, Joint convention of four electrical institutes, Res. Rep. Chiba Inst. Technol. (Sci. Technol.). 16 (1971) 22–31. https://www.scopus.com/inward/record.uri?eid=2-s2.0-78650297902&partnerID=40&md5=bac7c681de7a4731ee3b76447fe9916f.
[66] T. Ozawa, A New Method of Analyzing Thermogravimetric Data, Bull. Chem. Soc. Jpn. 38 (1965) 1881–1886, https://doi.org/10.1246/bcsj.38.1881.
[67] A. Zaker, Z. Chen, M. Zaheer-Uddin, J. Guo, Co-pyrolysis of sewage sludge and low-density polyethylene – A thermogravimetric study of thermo-kinetics and thermodynamic parameters, J. Environ. Chem. Eng. 9 (2021) 104554, https://doi.org/10.1016/j.jece.2020.104554.
[68] M.A. Mehmood, G. Ye, H. Luo, C. Liu, S. Malik, I. Afzal, J. Xu, M.S. Ahmad, Pyrolysis and kinetic analyses of Camel grass (Cymbopogon schoenanthus) for bioenergy, Bioresour. Technol. 228 (2017) 18–24, https://doi.org/10.1016/j.biortech.2016.12.096.
[69] J.W. Cumming, Reactivity assessment of coals via a weighted mean activation energy, Fuel 63 (1984) 1436–1440, https://doi.org/10.1016/0016-2361(84)90353-3.
[70] W.H. Chen, B.J. Lin, B. Colin, A. Pétrissans, M. Pétrissans, A study of hygroscopic property of biomass pretreated by torrefaction, Energy Procedia 158 (2019) 32–36, https://doi.org/10.1016/j.egypro.2019.01.030.
[71] A. Zheng, L. Jiang, Z. Zhao, Z. Huang, K. Zhao, G. Wei, X. Wang, F. He, H. Li, Impact of torrefaction on the chemical structure and catalytic fast pyrolysis behavior of hemicellulose, Lignin, and Cellulose, Energy Fuels 29 (2015) 8027–8034, https://doi.org/10.1021/acs.energyfuels.5b01765.
[72] B. Castells, I. Amez, L. Medic, J. García-torrent, Torrefaction influence on combustion kinetics of Malaysian oil palm wastes, Fuel Process. Technol. 218 (2021) 106843, https://doi.org/10.1016/j.fuproc.2021.106843.
[73] D. Nhuchhen, P. Basu, B. Acharya, A Comprehensive Review on Biomass Torrefaction, Int. J. Renew. Energy Biofuels. 2014 (2014) 1–56, https://doi.org/10.5171/2014.506376.
[74] J. Cai, W. Wu, R. Liu, G.W. Huber, A distributed activation energy model for the pyrolysis of lignocellulosic biomass, Green Chem 15 (2013) 1331–1340, https://doi.org/10.1039/c3gc36958g.
[75] B. Janković, V. Dodevski, I. Radović, M. Pijovi, Physico-chemical characterization of carbonized apricot kernel shell as precursor for activated carbon preparation in clean technology utilization, 236 (2019). https://doi.org/10.1016/j.jclepro.2019.117614.
[76] N. Nwabunwanne, T. Vuyokazi, A. Olagoke, O. Mike, M. Patrick, O. Anthony, Torrefaction Characteristics of Blended Ratio of Sewage Sludge and Sugarcane Bagasse for Energy Production, Appl. Sci. 11 (2021), https://doi.org/10.3390/app11062654.
[77] K. Świechowski, M. Hnat, P. Stępień, S. Stegenta-Dąbrowska, S. Kugler, J.A. Koziel, A. Białowiec, Waste to energy: solid fuel production from biogas plant digestate and sewage sludge by torrefaction-process kinetics, Fuel Properties, Energy Balance, Energies 13 (2020), https://doi.org/10.3390/en13123161.
[78] H.C. Ong, K.L. Yu, W.-H. Chen, M.K. Pillejera, X. Bi, K.-Q. Tran, A. Pétrissans, M. Pétrissans, Variation of lignocellulosic biomass structure from torrefaction: a critical review, Renew. Sustain. Energy Rev. 152 (2021) 111698, https://doi.org/10.1016/j.rser.2021.111698.
[79] Y. Lin, Y. Liao, Z. Yu, S. Fang, Y. Lin, Y. Fan, X. Peng, X. Ma, Co-pyrolysis kinetics of sewage sludge and oil shale thermal decomposition using TGA–FTIR analysis, Energy Convers. Manag. 118 (2016) 345–352, https://doi.org/10.1016/j.enconman.2016.04.004.
[80] A. Saddawi, J.M. Jones, A. Williams, C.Le Coeur, Commodity fuels from biomass through pretreatment and torrefaction: effects of mineral content on torrefied fuel characteristics and quality, Energy and Fuels 26 (2012) 6466–6474, https://doi.org/10.1021/ef2016649.
[81] N. Yaacob, N.A. Rahman, S. Matali, S.S. Idris, A.B. Alias, An overview of oil palm biomass torrefaction: effects of temperature and residence time, IOP Conf. Ser. Earth Environ. Sci. 36 (2016), https://doi.org/10.1088/1755-1315/36/1/012038.
[82] J. Poudel, T.I. Ohm, S.C. Oh, A study on torrefaction of food waste, Fuel 140 (2015) 275–281, https://doi.org/10.1016/j.fuel.2014.09.120.
[83] G. Jiang, L. Wei, Analysis of Pyrolysis Kinetic Model for Processing of Thermogravimetric Analysis Data, Phase Chang. Mater. Their Appl. (2018), https://doi.org/10.5772/intechopen.79226.
[84] S. Ren, H. Lei, L. Wang, Q. Bu, S. Chen, J. Wu, Thermal behaviour and kinetic study for woody biomass torrefaction and torrefied biomass pyrolysis by TGA, Biosyst. Eng. 116 (2013) 420–426, https://doi.org/10.1016/j.biosystemseng.2013.10.003.
[85] H. Kim, S. Yu, H. Ra, S. Yoon, C. Ryu, Prediction of pyrolysis kinetics for torrefied biomass based on raw biomass properties and torrefaction severity, Energy 278 (2023) 127759, https://doi.org/10.1016/j.energy.2023.127759.
[86] C. Chen, B. Qu, W. Wang, W. Wang, G. Ji, A. Li, Rice husk and rice straw torrefaction: properties and pyrolysis kinetics of raw and torrefied biomass, Environ. Technol. Innov. 24 (2021) 101872, https://doi.org/10.1016/j.eti.2021.101872.
[87] D.A. Granados, P. Basu, D.R. Nhuchhen, F. Chejne, Investigation into torrefaction kinetics of biomass and combustion behaviors of raw, torrefied and char samples, Biofuels 12 (2021) 633–643, https://doi.org/10.1080/17597269.2018.1558837.
[88] H. Liu, G. Xu, G. Li, Pyrolysis characteristic and kinetic analysis of sewage sludge using model-free and master plots methods, Process Saf. Environ. Prot. 149 (2021) 48–55, https://doi.org/10.1016/j.psep.2020.10.044.
[89] J. Wielinski, C. Müller, A. Voegelin, E. Morgenroth, R. Kaegi, Combustion of Sewage Sludge: kinetics and Speciation of the Combustible, Energy Fuels 32 (2018) 10656–10667, https://doi.org/10.1021/acs.energyfuels.8b02106.
[90] L. Gašparovič, Z. Koreňová, Ľ. Jelemenský, Kinetic study of wood chips decomposition by TGA, 64 (2010) 174–181. :10.2478/s11696-009-0109-4.
[91] A. Petrovič, S. Vohl, T. Cenčič Predikaka, R. Bedoić, M. Simonič, I. Ban, L. Čuček, Pyrolysis of solid digestate from sewage sludge and lignocellulosic biomass: kinetic and thermodynamic analysis, characterization of biochar, Sustain 13 (2021), https://doi.org/10.3390/su13179642.
[92] E. Díaz, L. Pintado, L. Faba, S. Ordóñez, J.M. González-LaFuente, Effect of sewage sludge composition on the susceptibility to spontaneous combustion, J. Hazard. Mater. 361 (2019) 267–272, https://doi.org/10.1016/j.jhazmat.2018.08.094.
[93] B. Castells, A. Varela, F.J. Castillo-Ruiz, L.F. Calvo, L. Medic, A. Tascón, Ignition and explosion characteristics of olive-derived biomasses, Powder Technol. 420 (2023) 118386, https://doi.org/10.1016/j.powtec.2023.118386.
[94] N. Manić, B. Janković, D. Stojiljković, M. Radojević, B.C. Somoza, L. Medić, Self-ignition potential assessment for different biomass feedstocks based on the dynamic thermal analysis, Clean. Eng. Technol. 2 (2021) 100040, https://doi.org/10.1016/j.clet.2020.100040.